

A MODIFIED GAUSSIAN FUNCTION FOR MODELING MAGNETIC HYSTERESIS UNDER DYNAMIC CONDITIONS

MOURAD DAFRI^{1,2*}, MOURAD NAIDJI¹, ABDELAZIZ LADJIMI², Wafa TOURAB¹, ABDELHAMID KSENTINI¹

Keywords: Preisach model; Magnetic hysteresis; Modified Gaussian distribution; Particle swarm optimization (PSO); NiFe₂O₄; Dynamic effects; Frequency; Temperature.

This paper presents a novel modified Gaussian distribution for the Preisach model to improve magnetic hysteresis modeling. Unlike classical distributions, the proposed approach incorporates additional parameters that provide a more accurate representation of the dispersion of elementary relay switching thresholds. The influence of each parameter on the hysteresis loop shape is analyzed in detail. The model parameters are identified using the particle swarm optimization (PSO) method, based on experimental data. The simulation results are then compared with experimental measurements on a NiFe₂O₄ ferrite, accounting for dynamic effects due to temperature and frequency. The results show that the proposed model provides good agreement between simulation and experiment, particularly regarding the width and slope of the hysteresis loops.

1. INTRODUCTION

Magnetic hysteresis is a fundamental phenomenon in ferromagnetic and ferrimagnetic materials, directly influencing the design and efficiency of electromagnetic devices such as transformers, electric motors, and sensors [1–5]. Accurate modeling of this behavior is essential for optimizing material performance and minimizing energy losses. Among the most used models, the Preisach model has emerged as a powerful tool to describe hysteresis by relying on a distribution function of the switching thresholds of elementary relays. This density can be identified not only from one or more experimental hysteresis loops [6–9] but also modeled using analytical functions such as the Lorentz or Cauchy function [10, 11], the modified Lorentz function [12], the Student function [13], or the Gaussian function [14].

In its traditional formulation, the two-dimensional Gaussian distribution is often employed to describe the distribution of switching thresholds. However, this approach imposes a symmetric dispersion that fails to capture certain asymmetric behaviors observed in real ferromagnetic materials. This limitation can lead to significant discrepancies between simulations and experimental measurements, particularly regarding the width and slope of hysteresis loops. Moreover, dynamic effects, such as frequency- and temperature-dependence, are not accounted for in this formulation, even though they play a crucial role in industrial applications where materials are subjected to environmental variations and high-frequency or temperature excitations.

To overcome these limitations, this paper proposes a novel modified Gaussian distribution for the Preisach model. This approach introduces additional parameters to improve the accuracy of the model by more finely adjusting the dispersion of switching thresholds. The objective is to better represent the diversity of hysteresis loops observed experimentally and to integrate dynamic effects related to frequency [15–18] and temperature [19–23]. This new formulation provides greater flexibility to capture loop asymmetries and enables more accurate modeling of materials operating under variable conditions.

To validate this approach, the model parameters are identified using the Particle Swarm Optimization (PSO) method [24–25], ensuring precise fitting of simulated curves.

The results are then compared with hysteresis cycles measured on magnetic materials, particularly ferrites, to assess the relevance of the proposed model at different temperatures and frequencies.

The results demonstrate the advantages of the proposed distribution function, showing a marked improvement in the agreement between simulations and experimental data.

2. PREISACH MODEL AND MODIFIED GAUSSIAN DISTRIBUTION

2.1 OVERVIEW OF THE CLASSICAL PREISACH MODEL

The classical Preisach model is based on the superposition of elementary hysteretic operators, called hysterons, each characterized by two switching thresholds α and β ($\alpha \geq \beta$). These thresholds define the up-switching and down-switching fields of an ideal two-state relay (ON/OFF), as illustrated in (Fig. 1). The hysterons are weighted by a probability density function $\rho(\alpha, \beta)$, which determines the distribution of the thresholds in the (α, β) plane. The Preisach model is then expressed as [26]:

$$M(t) = \int \int \rho(\alpha, \beta) \phi_{\alpha\beta} [H(t)] d\alpha d\beta. \quad (1)$$

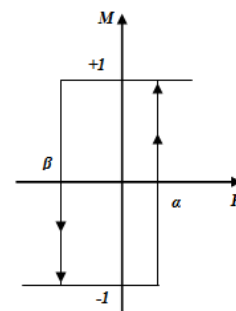


Fig. 1 – Elementary hysteresis loop of a magnetic entity.

where $\phi_{\alpha\beta} [H(t)]$ is the elementary hysteresis operator. The complete definition of the Preisach model requires prior knowledge of the Preisach distribution function. Therefore, it is essential to determine the final magnetization of the magnetic sample. Two main approaches are generally followed to identify this distribution function: the first is

¹ Electrical Engineering Department, Faculty of Engineering, Badji Mokhtari University, BP 12 Sidi Amar, Annaba 23000, Algeria.

² Laboratoire de Génie Électrique (LGEG), Université 8 Mai 1945 Guelma, BP. 401, Guelma, Algeria.

E-mails : mourad.dafri@univ-annaba.dz, mourad.naidji@univ-annaba.dz, ladjimi.abdelaziz@univ-guelma.dz, wafa.tourab@univ-annaba.dz, abdelhamid.ksentini@univ-annaba.dz

based on the analysis of a single experimental hysteresis loop or a set of loops, while the second relies on an analytical expression.

2.2. PROPOSAL AND JUSTIFICATION OF THE MODIFIED GAUSSIAN DISTRIBUTION

The new distribution is defined by a modification of the classical Gaussian law, designed to better represent dynamic phenomena and materials exhibiting an inhomogeneous dispersion of switching thresholds (α , β), and is given by

$$\rho(\alpha, \beta) = C \exp\left(-\lambda \frac{(\alpha - \alpha_0)^2}{H_c^2} - \lambda \frac{(\beta - \beta_0)^2}{H_c^2}\right), \quad (2)$$

where $\rho(\alpha, \beta)$ is the distribution density of the elementary operators; α and β represent the ascending and descending switching thresholds, respectively; α_0 et β_0 are the mean threshold values; with $\alpha_0 = \beta_0 \in [-H_s, H_s]$; H_c is the average coercive field, which determines the width of the hysteresis loop; λ is a tuning parameter controlling the spread of the distribution, with $\lambda > 0$; C is a normalization factor ensuring that the integral of the distribution is finite, with $C > 0$.

This modification of the distribution enables:

- A controlled asymmetry in the distribution of thresholds thereby improves the accuracy of the model for certain materials.
- A better adaptation to materials subjected to dynamic excitations, particularly under variations in temperature and frequency.
- An enhanced modeling of materials with an inhomogeneous dispersion of switching thresholds.

By incorporating this modified Gaussian distribution into the Preisach model, we aim to better capture dynamic effects and to render the model more realistic for the study of magnetic hysteresis in various ferromagnetic materials.

2.3. ADDITIONAL PARAMETERS INTRODUCED AND THEIR IMPACT ON THE HYSTERESIS LOOP

2.3.1 EFFECT OF THE PARAMETER λ ON THE HYSTERESIS LOOP

In this parametric study, the parameters C , α_0 , β_0 , and H_c are fixed, and the analysis is conducted by varying λ .

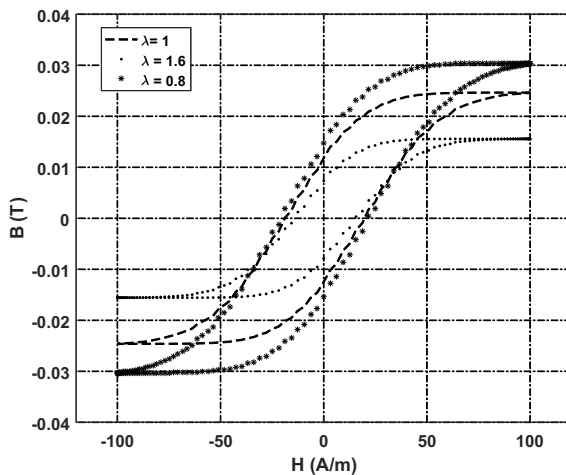


Fig. 2 – Hysteresis loop evolution under the influence of the parameter λ .

Figure 2 shows that variations in the parameter λ lead to significant changes in the characteristics of the hysteresis loop, such as the remanent induction (B_r), the saturation induction (B_s), the coercive field (H_c), as well as the slope of

the loop. This parameter, therefore, plays a crucial role in modeling, as it enables the reproduction of a wider range of hysteretic behaviors observed in different samples.

2.3.2 EFFECT OF THE PARAMETER C ON THE HYSTERESIS LOOP

In this parametric study, the parameters λ , α_0 , β_0 , and H_c are fixed, and the analysis is carried out by varying the normalization factor C .

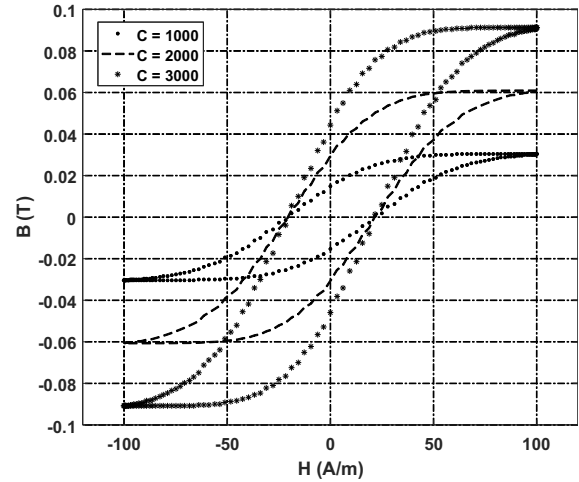


Fig. 3 – Hysteresis loop evolution under the influence of the parameter C .

Figure 3 shows that variations in the parameter C led to significant changes in the characteristics of the hysteresis loop, such as the remanent induction (B_r), the saturation induction (B_s), as well as the slope of the loop. This parameter, therefore, plays a crucial role in modeling, as it allows for the reproduction of a wider variety of hysteretic behaviors observed in different samples.

In conclusion, the introduction of new parameters into the modified Gaussian distribution has proven effective in improving the fitting of simulated hysteresis curves to experimental data. This approach not only enables a more accurate modeling of magnetic hysteresis phenomena but also provides better consideration of dynamic effects.

3. PARAMETER IDENTIFICATION AND OPTIMIZATION

The parameters of the modified Gaussian distribution associated with the hysteresis cycle are identified from experimental data, considering the ascending branch of the major loop, using a Particle Swarm Optimization (PSO)–based metaheuristic approach [27]. This method, previously validated for the identification of Preisach model parameters using a Student distribution [17], is adopted for its simplicity, robustness, and efficiency in solving complex nonlinear optimization problems. The identification procedure relies on minimizing the error between measured and simulated hysteresis loops through an iterative swarm-based optimization process, leading to an accurate and reliable estimation of the model parameters.

4. RESULTS AND DISCUSSION

4.1. MATERIALS AND EXPERIMENTAL PROTOCOL

The experimental sample consists of a toroidal core made of NiFe₂O₄ ferrite, which displays nonlinear hysteresis behavior. Its main properties are summarized in Table 1.

Table 1

Test sample characteristics: wound toroidal ferrite core NiFe_2O_4 .

NiFe ₂ O ₄ ferrite material	Diameter (outer diameter d_o and inner diameter d_i)	$d_o = 7.1\text{cm}$ $d_i = 5.7\text{cm}$
	Core Section	1.36 cm^2
	Mean length of the magnetic circuit (L_m)	12.72 cm
	Primary winding turns (N_1) and secondary winding turns (N_2)	$N_1 = 286\text{ turns}$ $N_2 = 143\text{ turns}$
	Maximum magnetic induction B_s	$B_s = 0.13\text{ T}$

The experimental setup consists of a ferrimagnetic core placed in a temperature-controlled chamber ($27\text{ }^\circ\text{C}$ – $160\text{ }^\circ\text{C}$) and excited by sinusoidal voltage at frequencies ranging from 1 Hz to 1 kHz. The magnetic field strength $H(t)$ and flux density $B(t)$ are derived from Ampère's and Faraday's laws, respectively, and recorded using a digital oscilloscope for post-processing. It should be noted that the voltage-controlled excitation leads to a non-strictly sinusoidal magnetic flux density, and the experiments are conducted at low flux density levels, below saturation. Consequently, the validity of the identified model parameters is limited to near-linear operating conditions (Fig. 4).

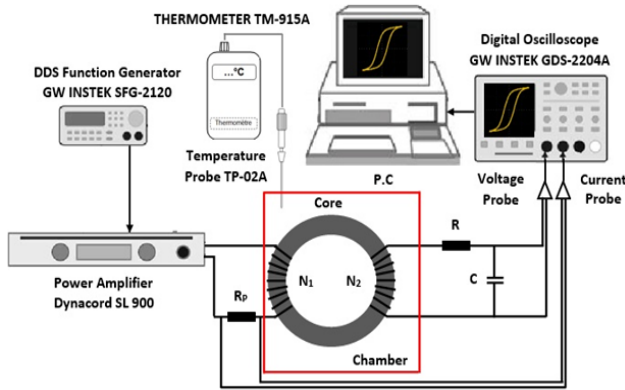


Fig. 4 Schematic of the experimental setup.

4.2. INVESTIGATION OF THE EFFECT OF TEMPERATURE

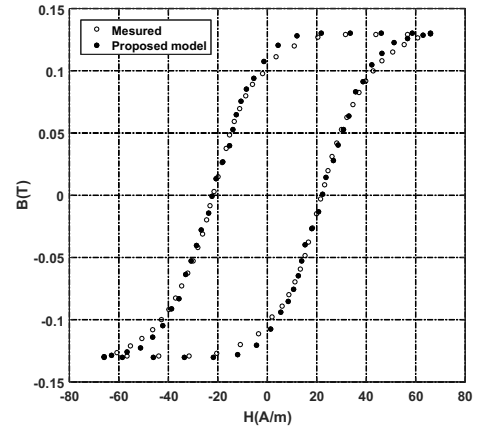
To validate the developed model, hysteresis loops were measured experimentally at five temperatures: $25\text{ }^\circ\text{C}$, $50\text{ }^\circ\text{C}$, $75\text{ }^\circ\text{C}$, $125\text{ }^\circ\text{C}$, and $150\text{ }^\circ\text{C}$, covering a representative thermal range for ferrimagnetic materials. At each stabilized temperature, a complete loop was recorded at 200 Hz, enabling comparison between experimental data and the Preisach model with the modified Gaussian distribution. This procedure assesses the model's ability to capture thermal effects on coercivity and magnetic saturation.

For each temperature, the parameters of the modified Gaussian distribution λ , $\alpha_0 = \beta_0$, and C in the Preisach model were identified using the PSO algorithm. The results of the model parameter identification at each temperature are summarized in Table 2.

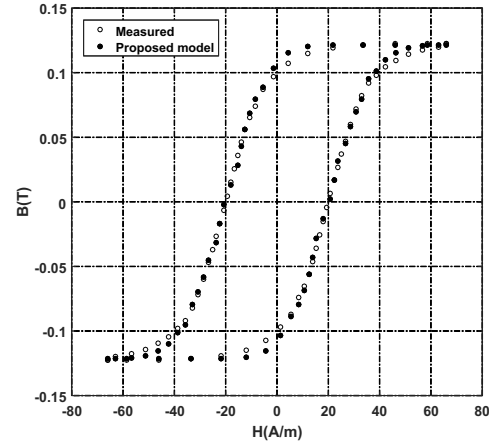
Table 2

Evolution of the distribution function parameters for each temperature.

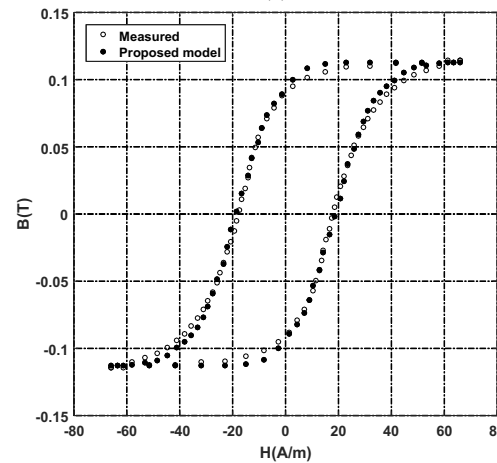
$T\text{ (}^\circ\text{C)}$	λ	$\alpha_0 = \beta_0$	C
27	0.70712	12.29373	3814587.57061
50	0.82827	11.69479	4979498.80142
75	0.60724	9.81493	4196835.49789
125	0.31063	4.22182	3836687.48298
150	0.23441	2.58660	3238316.15490



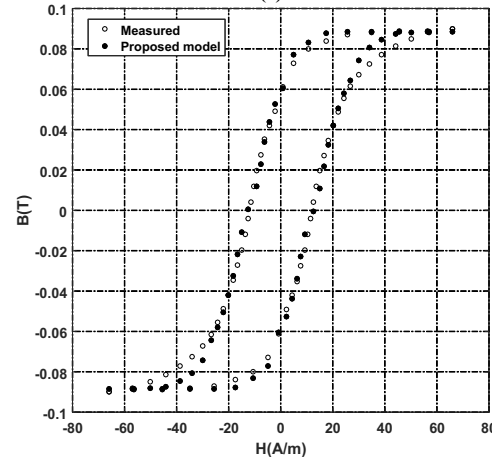
(a)



(b)



(c)



(d)

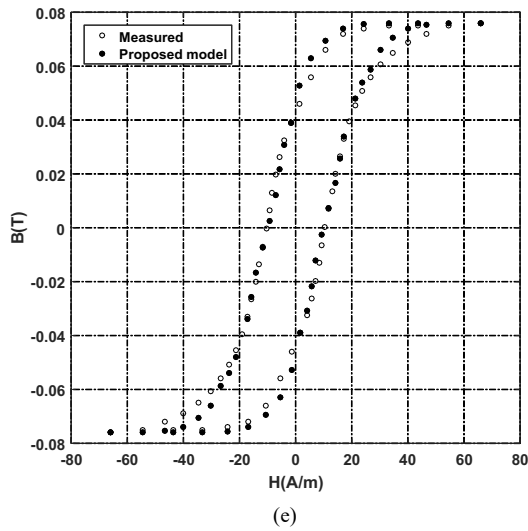


Fig. 5 – Comparison of measured and simulated hysteresis loops at multiple temperatures: (a) 27°C, (b) 50°C, (c) 75°C, (d) 125°C, and (e) 150°C

Table 3

Comparison of simulated and experimental results across different temperatures.

Temperature (°C)	B_s (T) (Measured/Simulated)	B_r (T) (Measured/Simulated)	H_c (A/m) (Measured/Simulated)	Global cycle error (%)
27	0.1300/0.1295	0.1024/0.1106	21.8998/22.1977	0.053
50	0.1225/0.1215	0.0993/0.1061	19.9852/20.4484	0.042
75	0.1143/0.1127	0.0903/0.0924	17.9696/18.9253	0.065
125	0.0900/0.0886	0.0581/0.0585	11.8985/12.5369	0.043
150	0.0760/0.0759	0.0430/0.0469	10.4175/10.7665	0.033

The results demonstrate excellent agreement between experimental and simulated data over the full temperature range. The overall error remains below 0.065 %, confirming the model's accuracy. The expected decrease in H_c , B_r , and B_s with rising temperature is well captured by the simulation.

4.3. INVESTIGATION OF THE EFFECT OF FREQUENCY

For further validation, hysteresis loops were measured at four frequencies (200 Hz, 400 Hz, 600 Hz, and 800 Hz), covering a range representative of practical operating conditions. All measurements were conducted at 27 °C to eliminate thermal effects and allow a precise comparison with simulations. This study assesses the model's robustness in reproducing dynamic effects caused by increasing frequency, including additional losses and changes in magnetic behavior. Parameter identification was carried out using the same material, the PSO method. The identified parameters and associated errors for each frequency are summarized in Table 4.

Table 4

Frequency-dependent evolution of the distribution function parameters.			
f (Hz)	λ	$\alpha_0 = \beta_0$	C
200	0.29114	5.99103	1216600.67644
400	0.39679	-10.35284	1233054.38096
600	0.40473	-10.9888	1078008.89378
800	0.44466	-13.01470	1034320.35984

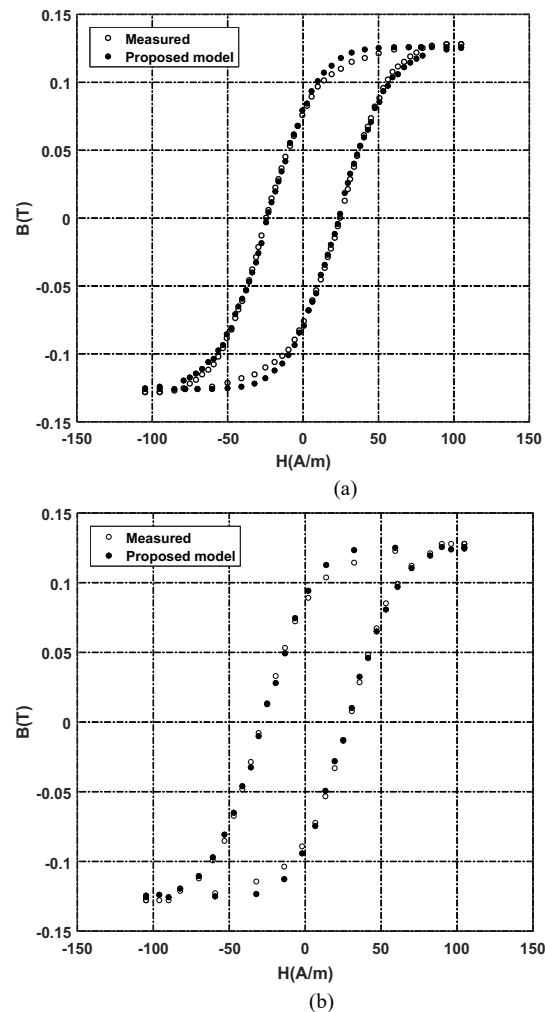
The curves shown in Fig. 6 represent the comparison between simulation results and experimental data for the evolution of the hysteresis loop at the operating frequencies of 200 Hz, 400 Hz, 600 Hz, and 800 Hz. These results confirm that the proposed model has been validated using experimental data from a ferrite material, NiFe₂O₄.

The curves shown in Fig. 5 represent the comparison between simulation results and experimental data for the evolution of the hysteresis loop at the operating temperatures of 27 °C, 50 °C, 75 °C, 125 °C, and 150 °C at a frequency of 200 Hz. These results confirm that the proposed model has been validated using experimental data from a ferrite material, NiFe₂O₄.

Table 3 reports the measured and simulated values of saturation induction B_s , remanent induction B_r , and coercive field H_c at different temperatures. The differences between measured and simulated values are minimal, indicating an overall acceptable error in the hysteresis loop. The root mean square error E between the measured and calculated magnetic inductions is calculated by equation 3.

$$E = \sqrt{\frac{\sum_{j=1}^n (B_{mj} - B_{cj})^2}{n}}, \quad (3)$$

where B_{mj} is the measured magnetic induction, B_{cj} is the magnetic induction calculated by the proposed model, and n is the number of measurement points.



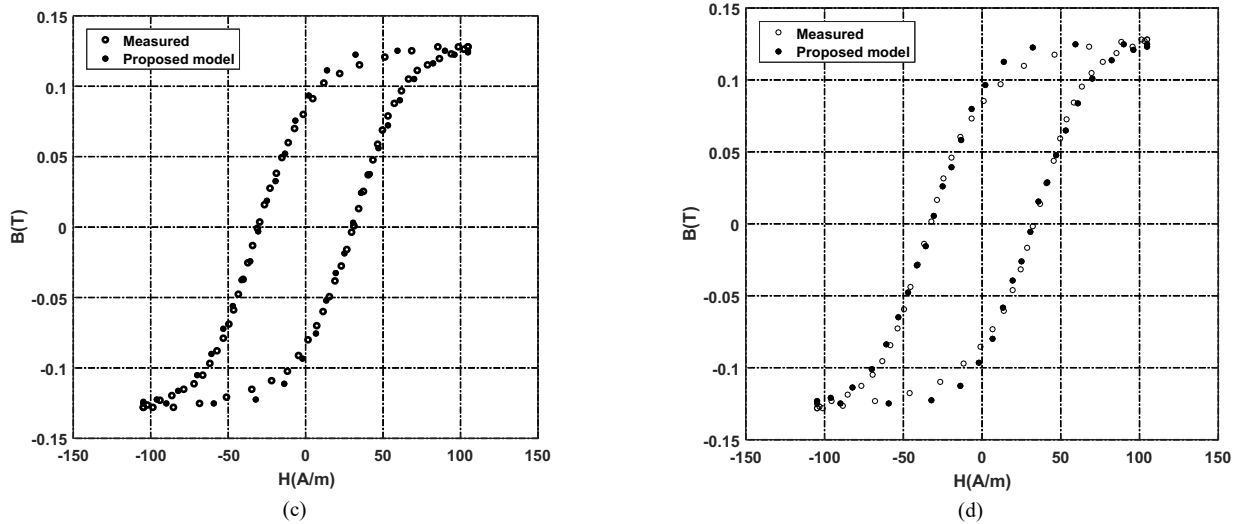


Fig. 6 – Experimental and simulated hysteresis loops across various frequencies: (a) 200 Hz, (b) 400 Hz, (c) 600 Hz, and (d) 800Hz.

Table 5 compares the measured and simulated values of the saturation induction B_s , remanent induction B_r , and coercive field H_c at different frequencies. These results demonstrate the

effectiveness of our model, with an excellent agreement between measured and simulated values across all frequencies.

Table 5
Comparison of simulated and experimental results across different frequencies.

Frequency (Hz)	B_s (T) (Measured/Simulated)	B_r (T) (Measured/Simulated)	H_c (A/m) (Measured/Simulated)	Global cycle error (%)
200	0.128 / 0.1257	0.0773 / 0.0801	24.61 / 23.93	0.066
400	0.128 / 0.1254	0.0851 / 0.0895	28.49 / 28.04	0.034
600	0.128 / 0.1253	0.0832 / 0.0885	30.79 / 30.11	0.062
800	0.128 / 0.1250	0.0839 / 0.0913	32.91 / 32.03	0.076

The measured and simulated values are very close, and the errors for each cycle remain low. The overall error remains below 0.076 %, confirming the model's reliability. Small deviations are observed mainly in B_r , whereas B_s and H_c are accurately reproduced.

5. CONCLUSIONS

In this work, we proposed an improvement of magnetic hysteresis modeling through a modified Gaussian distribution within the Preisach model, aiming to better represent the hysteretic behavior of magnetic materials under varying conditions. The Particle Swarm Optimization (PSO) algorithm was used to accurately identify the model parameters at different temperatures and frequencies, ensuring good agreement with experimental data.

The results demonstrate that the model can faithfully reproduce hysteresis loops while accounting for thermal and frequency effects. The flexibility provided by the modified distribution allows better adaptation to the material's physical characteristics, particularly for NiFe₂O₄ ferrites.

This study confirms the robustness and relevance of the proposed model for advanced modeling of magnetic materials, with potential applications in modern electromagnetic systems. Future work could extend this approach to other types of materials and incorporate additional effects, such as flux density dependence, thermo-mechanical phenomena, and other factors influencing magnetic properties.

ACKNOWLEDGMENT

This work was supported by the Directorate General for Scientific Research and Technological Development (DG-

RSDT) of Algeria

CREDIT AUTHORSHIP CONTRIBUTION STATEMENT

All the authors contribute equally to this paper.

Received on 23 September 2025

REFERENCES

- M.N. Benallal, A. Mahieddine, C.K. Khelil, A. Mazouz, *Use of the BH curves approximation for the calculation of magnetic circuits in electrical machines*, Rev. Roum. Sci. Techn. – Électrotechn. et Énerg., **68**, 1, pp. 42–45 (2023).
- S. Gao, Y. Li, H. Zhang, J. Tian, *A decoupled magnetic integration technique for dual-frequency topologies*, Rev. Roum. Sci. Techn. – Électrotechn. et Énerg., **69**, 2, pp. 153–158 (2024).
- O. Craiu, T.-I. Ichim, *Comparison of two bi-phase hybrid stepper motors, one with a solid and the other with a laminated stator*, Rev. Roum. Sci. Techn. – Électrotechn. et Énerg., **70**, 2, pp. 181–186 (2025).
- T. Tudorache, *Finite element analysis of a flexible dual-speed salient pole synchronous machine*, Rev. Roum. Sci. Techn. – Électrotechn. et Énerg., **70**, 1, pp. 21–26 (2025).
- O. Toudert, F. Auger, A. Houari, M. Laghrouche, *Novel rotor position extraction based on rotating high-frequency voltage injection for permanent magnet synchronous machine drives at low or zero speeds*, Rev. Roum. Sci. Techn. – Électrotechn. et Énerg., **68**, 2, pp. 188–193 (2023).
- I.D. Mayergoyz, *Mathematical models of hysteresis*, Elsevier, pp. 1–300 (2003).
- I.D. Mayergoyz, *Mathematical models of hysteresis and their applications*, IEEE Trans. Power Systems, pp. 1–10 (1992).
- Y. Bernar, E. Mendes, Z. Ren, *A new method for the determination of the parameters in Preisach model*, CEFC'98, Tucson, Arizona, USA, pp. 1–6 (1998).
- S. Clénet, F. Piriou, *Identification de la fonction d'Everett pour le modèle de Preisach*, MGE 2000, Lille, France, pp. 71–74 (2000).
- G. Bertotti, V. Basso, *Considerations on the physical interpretation of the Preisach model of ferromagnetic hysteresis*, Journal of Applied

- Physics, pp. 1–10 (1993).
11. P. Pruksanubal, A. Binner, K.H. Gonschorek, *Modeling of magnetic hysteresis using Cauchy distribution*, 3rd International Symposium on Electromagnetic Compatibility, pp. 446–449 (2002).
 12. Y.O. Amor, M. Féliachi, *Présentation d'une fonction de Lorentz modifiée pour une modélisation de l'hystérésis magnétique*, Colloque MGE 2000 sur les matériaux du génie électrique, Lille, France, pp. 1–6 (2000).
 13. M. Dafri, A. Lajimi, S. Mendaci, A. Babouri, *Modeling of magnetic hysteresis using Student distribution*, J. Supercond. Nov. Magn., pp. 1–10 (2020).
 14. F. Delincé, *Modélisation des régimes transitoires dans les systèmes comportant des matériaux magnétiques non linéaires et hystérétiques*, Ph.D. dissertation, Faculté des Sciences Appliquées de Liège, pp. 1–200 (1994).
 15. G. Bertotti, *Dynamic generalization of the scalar Preisach model of hysteresis*, IEEE Transactions on Magnetics, **28**, 5, pp. 2599–2601 (1992).
 16. Y. Bernard, E. Mendes, F. Bouillault, *Dynamic hysteresis modeling based on Preisach model*, IEEE Transactions on Magnetics, **38**, 2, pp. 885–888 (2002).
 17. A. Ladjimi, M. Dafri, S. Fisli, *Phenomenological model of the frequency-dependent hysteresis of ferrite NiFe₂O₄*, Rev. Roum. Sci. Techn. – Électrotechn. et Énerg., **67**, 3, pp. 275–279 (2022).
 18. A. Ladjimi, A. Babouri, *Modeling of frequency effects in a Jiles-Atherton magnetic hysteresis model*, Rev. Roum. Sci. Techn. – Électrotechn. et Énerg., **61**, pp. 217–220 (2016).
 19. S.H. Ould Ouali, H. Mohelleb, R. Chaïbi, M. Féliachi, *Introduction de l'effet de la température dans le modèle de Preisach pour la génération des cycles d'hystérésis*, J. Phys. IV France, **124**, pp. 315–320 (2005).
 20. H. Chen, Q. Xu, Y. Xiang, Y. Huang, *Temperature characteristics modeling of Preisach theory*, MATEC Web of Conferences, **139**, pp. 1–6 (2017).
 21. T. Monnor, K. Kanchiang, R. Yimnirun, Y. Laosiritaworn, *Preisach modeling on temperature-dependent mean-field Ising-hysteresis*, Ferroelectrics, **459**, 1, pp. 128–133 (2014).
 22. M. Dafri, A. Ladjimi, S. Mendaci, A. Babouri, *Phenomenological model of the temperature dependence of hysteresis based on the Preisach model*, J. Supercond. Nov. Magn., **34**, pp. 1453–1458 (2021).
 23. H. Zhang, Q. Yang, C. Zhang, Y. Li, Y. Chen, *Temperature-dependent hysteresis model based on temporal convolutional network*, AIP Advances, **14**, 2, pp. 1–10 (2024).
 24. R. Eberhart, J. Kennedy, *A new optimizer using particle swarm theory*, MHS'95. Proceedings of the Sixth International Symposium on Micro Machine and Human Science, Nagoya, Japan, pp. 39–43 (1995).
 25. L. Chen, Q. Yi, T. Ben, Z. Zhang, Y. Wang, *Parameter identification of Preisach model based on velocity-controlled particle swarm optimization method*, AIP Advances, **11**, pp. 1–10 (2021).
 26. F. Preisach, *Über die magnetische Nachwirkung*, Zeitschrift für Physik, pp. 1–10 (1935).
 27. R. Marion, R. Scorretti, N. Siauve, M. Raulet, L. Krahenbuhl, *Identification of Jiles-Atherton model parameters using particle swarm optimization*, IEEE Transactions on Magnetics, **44**, 6, pp. 894–897 (2008).